MODELING FISSION GAS RELEASE AND BUBBLE EVOLUTION IN UO_2 FOR ENGINEERING FUEL ROD ANALYSIS

G. PASTORE
Fuel Modeling and Simulation Department, Idaho National Laboratory
P.O. Box 1625, Idaho Falls, ID 83415-3840, United States

T. BARANI, D. PIZZOCRI, A. MAGNI, L. LUZZI
Politecnico di Milano, Department of Energy, Nuclear Engineering Division
via La Masa 34, 20156 Milano, Italy

ABSTRACT

We present model developments for fission gas behavior and application to integral fuel rod simulations with the BISON fuel performance code. First, we give an overview of a physics-based engineering model of fission gas behavior developed in recent years and available in BISON. The model includes the fundamental physical processes of intra-granular bubble evolution and swelling coupled to gas atom diffusion, bubble evolution and swelling at grain boundaries, fission gas release due to grain-boundary bubble interconnection and micro-cracking during transients. Second, we present recent BISON simulations of LWR fuel rod irradiation tests including power ramps from the Risø-3 experiment. Calculations are compared to post-irradiation experimental data of fission gas release, xenon radial distributions in the fuel, and cladding diameter profiles. These new results extend the experimental validation base of the fission gas model for integral fuel rod simulations.

1. Introduction

Nuclear fuel of most present-day commercial Light Water Reactors (LWR) consists of zirconium-alloy cladding tubes filled with sintered cylindrical UO_2 fuel pellets characterized by a granular structure. Approximately 30% of the fission products created during the irradiation are isotopes of xenon and krypton. These fission gases dissolve poorly in the UO_2 matrix and form bubbles inside and on the boundary of grains, or are ultimately released to the fuel-to-cladding gap and plenum. Fission gas behavior significantly alters the thermo-mechanical performance of the nuclear fuel rods. Fuel swelling due to gas bubbles promotes pellet-cladding mechanical interaction (PCMI), and fission gas release (FGR) increases the rod internal pressure, both processes affecting the mechanical behavior of the cladding. Moreover, gas release and bubble evolution affect the gap thermal conductance and the fuel thermal conductivity, respectively, and consequently the temperature distribution in the fuel [1-3].

It follows that the calculation of fission gas swelling and release is an important part of engineering fuel rod analysis, and accurate physics-based models of fission gas behavior that can be effectively applied in fuel performance codes need to be developed. In recent years, we developed an efficient physics-based engineering model of fission gas release and gaseous swelling in UO_2 [4-7]. While it includes all fundamental physical processes of fission gas behavior, this model is characterized by a level of complexity that makes it suitable for application to integral fuel analysis and consistent with the uncertainties pertaining to some parameters. Fission gas release and gaseous swelling are modeled as inherently coupled. In this work we apply the model in BISON [8,9], a modern finite-element based, multidimensional fuel performance code developed at Idaho National Laboratory (INL).

This paper provides an overview of the fission gas model and recent results from BISON integral fuel rod simulations of irradiation tests from the Risø-3 experiment, including comparisons to experimental data of fission gas release and distribution in the fuel pellets, and rod mechanical behavior which is linked to gaseous swelling. The fission gas behavior model in BISON is summarized in Section 2. Fuel rod analyses and comparisons of the results to experimental data are presented in Section 3. Conclusions are drawn in Section 4.

2. Modeling

The model considered in this work was developed with the aim to incorporate in the thermo-mechanical analysis of the fuel a physics-based calculation of fission gas release and gaseous swelling while maintaining relatively low complexity and computational expense [4-7]. In addition, this model represents a means for the application to engineering-scale nuclear fuel performance analysis of the physical understanding developed through advanced lower-length scale calculations [10]. Such scale bridging requires a link to the physical mechanisms and cannot be achieved using empirical models.

The model includes physically based descriptions of gas behavior at the grain interior and grain boundaries. On this basis, it calculates the fission gas release and gaseous swelling concurrently, as inherently coupled processes. An overview of the model is provided in the following. The model is available in the BISON code. More detailed descriptions of model's characteristics can be found in [4-7].

2.1. Intra-granular behavior

The module for intra-granular fission gas behavior computes the coupled intra-granular bubble evolution and gas atom diffusion to grain boundaries [7]. Starting from a detailed cluster dynamics formulation, simplifications are applied to compute only the total number density and average size of the bubbles (hence, bubble swelling) along with the diffusion rate of single gas atoms to grain boundaries, while retaining a physical basis.

Defining the total number density of bubbles, N (m^{-3}), the total concentration of gas residing in bubbles, ψ (m^{-3}), and the average number of atoms per bubble $\bar{n} = \psi / N$, the final form of the model consists of only three differential equations, as follows:

$$\begin{aligned} \frac{\partial N}{\partial t} &= +\nu - \alpha_{\bar{n}} N \\ \frac{\partial \psi}{\partial t} &= +2\nu + \beta_{\bar{n}} N - \alpha_{\bar{n}} \psi \\ \frac{\partial c_1}{\partial t} &= +yF + D\nabla^2 c_1 - 2\nu - \beta_{\bar{n}} N + \alpha_{\bar{n}} \psi \end{aligned} \tag{1}$$

Here, t (s) is the time, y (/) is the yield of fission gas atoms, D ($m^2 s^{-1}$) the single atom diffusion coefficient, ν ($m^{-3} s^{-1}$) the rate of bubble (dimer) nucleation, β (s^{-1}) the rate of gas atom trapping at bubbles, α (s^{-1}) the re-solution rate, and the parameters α, β are calculated at $\bar{n}$. The average bubble radius is calculated as

$$R_{\bar{n}} = \left(\frac{3\Omega}{4\pi} \bar{n} \right)^{1/3} \tag{2}$$

with Ω (m^3) being the atomic volume in the bubble. For spherical bubbles, the swelling component due to intra- granular bubbles is at last

$$\left(\frac{\Delta V}{V} \right)_{ig} = \frac{4}{3} \pi R_{\bar{n}}^3 N \tag{3}$$

Note that the total intra-granular swelling is given by the sum of the contributions due to bubbles and dissolved fission products. Eq. (3) only accounts for swelling due to fission gas bubbles. As atoms are transferred from the solution to the bubbles, the matrix swelling due to dissolved fission gas decreases correspondingly.

The detailed derivation of the model is found in [7].

The diffusion equation is solved using a recently developed numerical algorithm that provides a high-accuracy solution combined with a low computational cost, as is necessary for application in integral codes [11].

2.2 Grain-boundary behavior and fission gas release

The grain-boundary gas behavior module entails a physics-based and coupled treatment of both fission gas swelling and release through a direct description of the grain-face bubble development. The main features of the model are as follows. More details are found in [4-6].
An initial number density of grain-face bubbles is considered, and further nucleation during irradiation is neglected (one-off nucleation). The absorption rate of gas atoms at grain-face bubbles is assumed equal to the arrival rate of gas at grain boundaries. All grain-face bubbles are considered to have, at any instant, equal size and equal lenticular shape of circular projection. Bubbles grow (or shrink) by inflow of gas atoms from within the grains and concomitant absorption (or emission) of vacancies from the grain boundaries. The vacancy absorption rate at bubbles is function of the excess bubble pressure relative to the mechanical equilibrium pressure:

$$\frac{dn_v}{dt} = \frac{2\pi D_v \delta_g}{kTs}\left(p - p_{eq}\right) \tag{4}$$

where n_v (-) is the number of vacancies per bubble, D_v (m^2s^{-1}) the vacancy diffusion coefficient along grain boundaries, δ_g (m) the thickness of the grain-boundary diffusion layer, k ($J \cdot K^{-1}$) the Boltzmann constant, T (K) the temperature, s (-) a parameter, p (Pa) the gas pressure in the bubble and p_{eq} (Pa) the mechanical equilibrium pressure [4,12]. The bubble volume is calculated through

$$\frac{dV_{gf}}{dt} = \omega \frac{dn_g}{dt} + \Omega \frac{dn_v}{dt} \tag{5}$$

where V_{gf} (m^3) is the bubble volume, ω (m^3) the Van der Waals covolume of a fission gas atom, n_g (–) the number of fission gas atoms per bubble, Ω (m^3) the atomic (vacancy) volume in the bubble, and n_v (–) the number of vacancies per bubble. The gas atom inflow rate at the bubble, dn_g/dt, is obtained from the intra-granular diffusion calculation included in Eq. (1). The fractional volume grain-face fission gas swelling is calculated as

$$\frac{\Delta V}{V} = \frac{1}{2}\frac{3}{a} N_{gf} V_{gf} \tag{6}$$

where V (m^3) is the fuel volume, a (m) the grain radius and N_{gf} (m^{-2}) the bubble number density. Grain-face bubble coalescence is considered through an improved model of White based on a geometrical reasoning for the rate of bubble mechanical interference on the grain surface during growth [4,12]. The total relative volume of the grain-face bubbles gives the corresponding contribution to fission gas swelling [4].
Bubble size is also affected by the gas escape term as FGR occurs. One component of thermal fission gas release considered in the model is associated with bubble growth and interconnection. This contribution is calculated based on a principle of grain face saturation. More precisely, when the fractional grain-face coverage of bubbles attains a saturation value, further bubble growth is compensated by gas release from the grain faces in order to maintain the saturation coverage condition:

$$\frac{dF_c}{dt} = \frac{d(N_{gf} A_{gf})}{dt} = 0 \qquad \text{if } F_c = F_{c,sat} \tag{7}$$

where F_c (/) is the fractional coverage, N_{gf} (m^{-2}) the number density of grain-face bubbles, A_{gf} (m^2) the bubble projected area, and $F_{c,sat}$ the saturation coverage. For intact grain faces, $F_{c,sat}$=0.5 [4,12].
Non-intact grain faces are also allowed for, in a representation of the additional FGR mechanism of grain face separation due to micro-cracking [6,13]. This mechanism is considered as responsible for the rapid FGR observed during transients (burst release) as it leads to gas depletion of the separated grain faces and correspondingly to increased FGR. This part of the model is semi-empirical. Gas depletion of a fraction of the grain faces is

modeled as a reduction of both the fractional and saturation coverages, effectively leading to a decrease of the amount of gas retained in the fuel (consequently, of local gaseous swelling) and to a corresponding increase of FGR. In particular, F_c and $F_{c,sat}$ are scaled by a factor, f (/), corresponding to the fraction of intact grain faces. To compute the time evolution of f, we observe that the micro-cracking process can only affect intact grain faces, and write

$$\left[\frac{df}{dt}\right]_c = -\frac{dm}{dt} f \tag{8}$$

where the subscript c stands for micro-cracking. Here, m is an empirical micro-cracking parameter that embodies the temperature dependence of the process. The functional form of m is chosen as a sigmoid function of temperature:

$$m(T) = 1 - \left[1 + Q \exp\left(z \frac{T - T_{infl}}{B}\right)\right]^{-\frac{1}{Q}} \tag{9}$$

where T_{infl} (K) is the value for the temperature at the inflection point of the function $m(T)$ (temperature of maximum micro-cracking rate), and B (K) and Q (–) are parameters related to the temperature-domain width of the phenomenon and the deviation from symmetric behavior during heating/cooling transients, respectively. The value of z (-) is set to +1 during heating transients and to –1 during cooling transients, so that m increases during both heating and cooling. Eqs. 4 and 5 combined lead to a FGR contribution that activates only during temperature variations in time (transients). Model's characteristics are based on the available experimental evidence of transient FGR and imply a continuous but peaked temperature-dependent release rate during transients. Burnup dependence of micro-cracking, and micro-crack healing, are also accounted for, although details are not given here for brevity (see [6,13] for a more extensive description of the model and references).
Athermal gas release as well as grain growth and grain boundary sweeping are also included in the model in BISON. Details are not dealt with here for brevity, and can be found in [14].
The model was implemented in the thermo-mechanics analysis framework of BISON to provide calculation of the fuel inelastic strain contribution due to gaseous swelling and the amount of gas released to the fuel-cladding gap and plenum, which in turn affects the gap thermal conductance and rod inner pressure.

3. Simulations of integral fuel rod experiments

The BISON code with the fission gas behavior model summarized in Section 2 was applied to simulations of LWR fuel rod irradiation tests involving power ramps from the Risø-3 experiment [15]. A description of the experiments and comparisons of the simulation results to the experimental data are given in the following. Comparisons are new and extend the validation base of the fission gas model for integral fuel rod analyses relative to previously published work [4,6,9].

3.1. Irradiation experiments

We simulated two integral irradiation tests of LWR fuel rods from the Risø-3 experiment [15]. Rods were base-irradiated in the BIBLIS A PWR (Germany) and ramp tested in the DR3 research reactor at Risø (Denmark) under PWR conditions. Specifically, the simulated irradiation experiments are the Risø-3 AN2 and AN8 tests. Rod average burnups after the commercial base irradiation were about 41.5 GWd·tU^{-1} for AN2 and about 42.3 GWd·tU^{-1} for AN8. The main fabrication characteristics of the fuel rods are given in Table 1. Both rods consisted of UO_2 fuel and Zircaloy-4 cladding. These experiments were selected based on the availability of experimental data allowing detailed comparisons to simulations results with specific reference to fission gas modeling. In particular, Post-Irradiation Examination (PIE) data for these experiments include measurements of FGR, radial Xe distribution in the fuel and cladding dimensional changes at the end of the test. More details on fuel fabrication data, irradiation conditions and PIE can be found in [15].

	Risø-3 AN2	Risø-3 AN8
Pellet outer diameter (mm)	9.05	9.05
Cladding inner diameter (mm)	9.26	9.26
Cladding outer diameter (mm)	10.80	10.81
Cladding wall thickness (μm)	775	772
Fuel stack length (mm)	541.8	541.8
Plenum length (mm)	60.96	60.96
Fill gas	He	He
Fill gas pressure (MPa)	2.31	2.31
Fuel grain size 2D (μm)	6	6
Enrichment (%)	2.95	2.95

Tab 1: Fabrication data of the fuel rods analyzed in the present work [15].

3.2 Results and discussion

The input average linear heat rate (LHR) and calculated integral FGR for the two fuel rod simulations, and the experimental FGR data point, are shown in Fig. 1. The integral FGR is defined as the ratio between the amounts of gas released and generated in the fuel rod. The agreement between the calculated FGR and the measured values at the end of life is good. More meaningfully, differences are within the inherent uncertainties in FGR calculations, which are significant [5]. The stepwise increments of FGR in correspondence of the power transients, including the final shut-downs, are associated with the transient (burst) release capability in the fission gas model (Section 2.2). These rapid increases are qualitatively consistent with the behavior experimentally observed in similar irradiation tests where on-line rod pressure measurements were performed [6,9,13-15].

Fig. 2 compares the BISON calculations to radial distributions of Xe in the fuel grains measured by Electron Probe Microanalysis (EPMA). Such local comparisons are possible for a fuel performance code with a physics-based model of fission gas behavior that includes direct modeling of the fundamental mechanisms. In particular, these comparisons showcase the recently developed intra-granular model presented in Section 2.1, coupled to the BISON global thermo-mechanics analysis. Calculated concentrations of intra-granular fission gas compare very well to the EPMA data. Note that the BISON calculations include Xe+Kr, which implies that a slight bias exists in the comparisons.

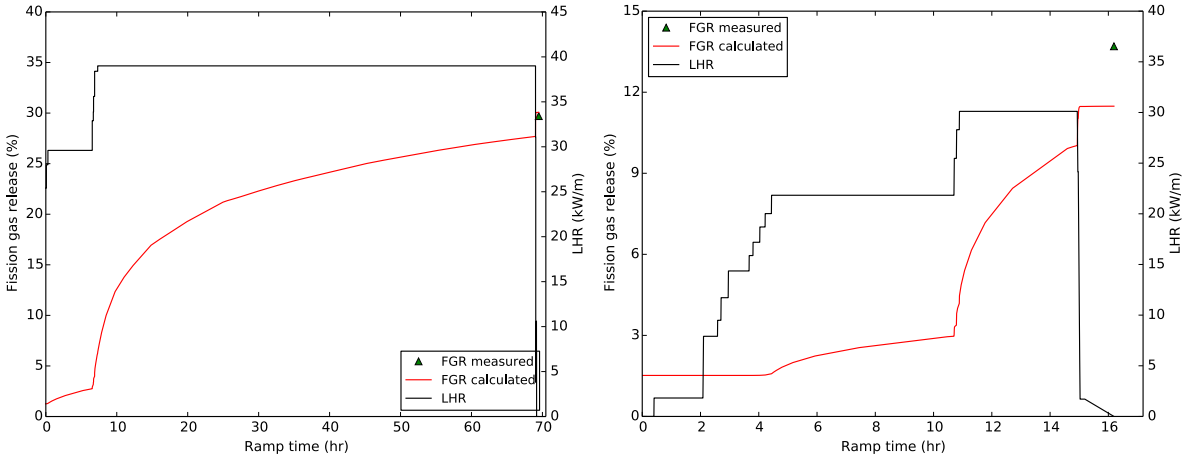

Fig 1: Integral fission gas release and rod average linear heat rate as a function of the time for the Risø-3 AN2 (left) and AN8 (right) tests. FGR simulation results and PIE data (puncturing) are illustrated. Time zero corresponds to the beginning of the ramp test.

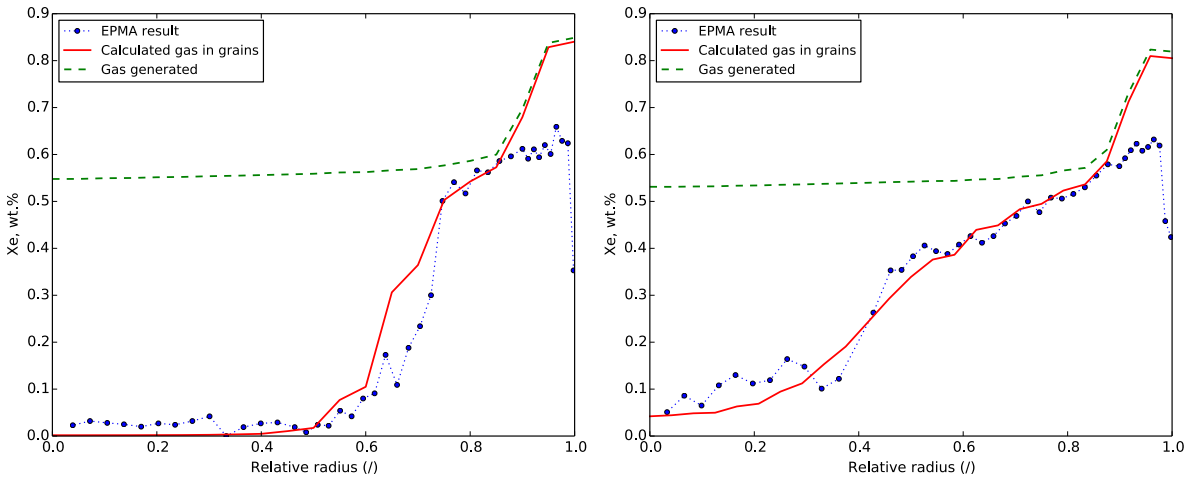

Fig 2: Radial distributions of Xe at the end of life (EOL) for the Risø-3 AN2 (left) and AN8 (right) cases. BISON calculations are compared to the PIE data (EPMA). Calculated profile of total gas generated is also included.

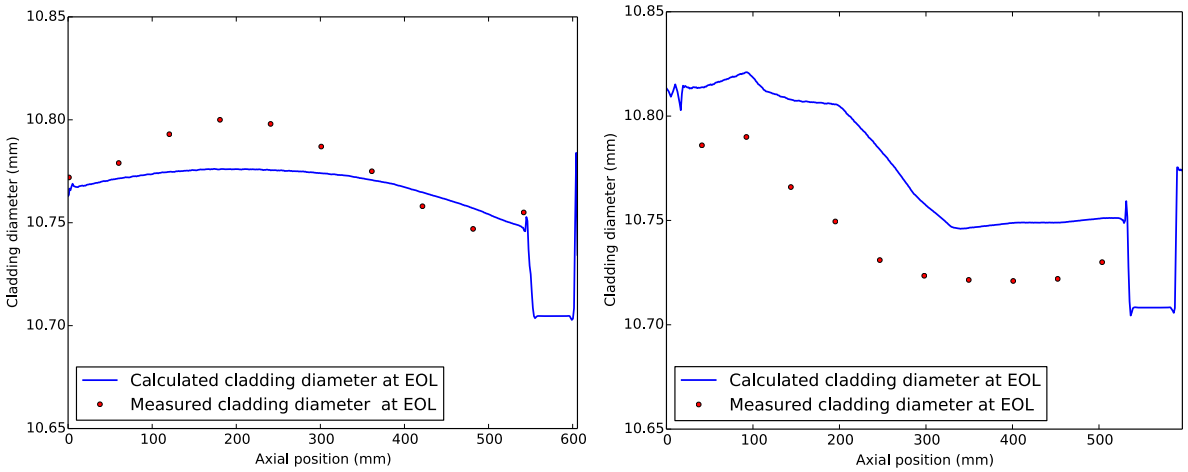

Fig 3: Cladding outer diameter as a function of the axial position at the end of life (EOL) for the Risø-3 AN2 (left) and AN8 (right) cases. BISON calculations are compared to the PIE data.

The over-prediction of the intra-granular gas concentration close to the pellet periphery may be associated with the formation of the high-burnup structure (HBS) and the associated fuel re-crystallization that leads to partial fission gas depletion of the grains [16]. This effect is currently not considered in the fission gas model, and will be the subject of future work.
Fig. 3 shows the calculated cladding outer diameter at the end of the tests as a function of the axial position along with the PIE data. Under PCMI conditions (as is the case during the ramp tests considered here), fission gas swelling along with thermal expansion of the fuel pellets drives cladding strain. Hence the importance of fission gas swelling in cladding diameter predictions. Indeed, the calculated cladding strain depends on several other processes, also including cladding thermal expansion, elasticity, creep and plasticity, and is therefore affected by various models. Comparisons in Fig. 3 point out maximum differences between the calculated and measured cladding diameter of about 30 μm for the AN2 case and about 50 μm for AN8. Also, the shape of the experimental cladding diameter profile appears to be reproduced correctly by BISON.

4. Conclusions

In this contribution, a physics-based model for the calculation of fission gas swelling and release in engineering fuel performance codes was summarized, and integral validation results for simulations of fuel rod experiments with the BISON code were presented. In

particular, two irradiation experiments involving power ramps from the Risø-3 experiment were simulated, and calculations were compared to experimental data.
Calculations of fission gas release at the EOL were in good agreement with the experimental data. More meaningfully, results were within the inherent uncertainties in FGR calculations. The calculated kinetics of FGR during the ramp tests involved rapid FGR increases during the transients as predicted with the burst release capability in the current model. This behavior is consistent with experimental observations for similar tests where on-line FGR measurements were performed. We also compared the calculated radial profiles of intra-granular Xe concentrations to the EPMA experimental data, showing a very good agreement overall. Discrepancies near the pellet periphery were ascribed to fission gas behavior in the HBS, which will be the subject of future developments. Finally, we compared BISON calculations to cladding diameter axial profiles at the end of the tests, demonstrating an encouraging accuracy of the predictions. The new experimental comparisons presented in this paper extend the validation base of the fission gas behavior model for integral fuel rod simulations relative to previously published work.

Acknowledgements

This work was funded by the U.S. Department of Energy Scientific Discovery through Advanced Computing (SciDAC) project on Simulation of Fission Gas and by the Nuclear Energy Advanced Modeling and Simulation (NEAMS) program.
The submitted manuscript has been authored by a contractor of the U.S. Government under Contract DE-AC07-05ID14517. Accordingly, the U.S. Government retains a non-exclusive, royalty-free license to publish or reproduce the published form of this contribution, or allow others to do so, for U.S. Government purposes.

References

[1] R.J. White, M.O. Tucker, A new fission-gas release model, *J. Nucl. Mater.* 118, 1-38 (1983).
[2] D.R. Olander, A.T. Motta, *Light Water Reactor Materials, Volume I: Fundamentals*, American Nuclear Society, LaGrange Park, IL, USA (2017).
[3] M. Tonks, D. Andersson, R. Devanathan, R. Dubourg, A. El-Azab, M. Freyss, F. Iglesias, K. Kulacsy, G. Pastore, S.R. Phillpot, M. Welland, Unit mechanisms of fission gas release: Current understanding and future needs, *J. Nucl. Mater.* 504, 300-317 (2018).
[4] G. Pastore, L. Luzzi, V. Di Marcello, P. Van Uffelen, Physics-based modelling of fission gas swelling and release in UO_2 applied to integral fuel rod analysis, *Nucl. Eng. Des.* 256, 75–86 (2013).
[5] G. Pastore, L.P. Swiler, J.D. Hales, S.R. Novascone, D.M. Perez, B.W. Spencer, L. Luzzi, P. Van Uffelen, R.L. Williamson, Uncertainty and sensitivity analysis of fission gas behavior in engineering-scale fuel modeling, *J. Nucl. Mater.* 456, 398-408 (2015).
[6] T. Barani, E. Bruschi, D. Pizzocri, G. Pastore, P. Van Uffelen, R.L. Williamson, L. Luzzi, Analysis of transient fission gas behaviour in oxide fuel using BISON and TRANSURANUS, *J. Nucl. Mater.* 486, 96–110 (2017).
[7] D. Pizzocri G. Pastore, T. Barani, A. Magni, L. Luzzi, P. Van Uffelen, S.A. Pitts, A. Alfonsi, J.D. Hales, A model describing intra-granular fission gas behaviour in oxide fuel for advanced engineering tools, *J. Nucl. Mater.* 502, 323-330 (2018).
[8] R.L. Williamson, J.D. Hales, S.R. Novascone, M.R. Tonks, D.R. Gaston, C.J. Permann, D. Andrs, R.C. Martineau, Multidimensional Multiphysics Simulation of Nuclear Fuel Behavior, *J. Nucl. Mater.* 423, 149-163 (2012).
[9] R.L. Williamson, K.A. Gamble, D.M. Perez, S.R. Novascone, G. Pastore, R.J. Gardner, J.D. Hales, W. Liu, A. Mai, Validating the BISON fuel performance code to integral LWR experiments, *J. Nucl. Mater.* 301, 232-244 (2016).
[10] Scientific Discovery through Advanced Computing (SciDAC-2) project on *Simulation of Fission Gas in Uranium Oxide Nuclear Fuel*, https://collab.cels.anl.gov/display/FissionGasSciDAC2.
[11] D. Pizzocri, C. Rabiti, L. Luzzi, T. Barani, P. Van Uffelen, G. Pastore, PolyPole-1: An accurate numerical algorithm for intra-granular fission gas release, *J. Nucl. Mater.* 478, 333-342 (2016).
[12] R.J. White, The development of grain-face porosity in irradiated oxide fuel, *J. Nucl. Mater.* 325, 61-77 (2004).

[13] G. Pastore, D. Pizzocri, J. Hales, S. Novascone, D. Perez, B. Spencer, R. Williamson, P. Van Uffelen, L. Luzzi, Modelling of transient fission gas behaviour in oxide fuel and application to the BISON code, in: Enlarged Halden Programme Group Meeting, Røros, Norway (2014).
[14] G. Pastore, J.D. Hales, S.R. Novascone, D.M. Perez, B.W. Spencer, R.L. Williamson, Analysis of fission gas release in LWR fuel using the BISON code, in: Proc. of the LWR Fuel Performance Meeting, Charlotte, NC, USA (2013).
[15] E. Sartori, J. Killeen, J.A. Turnbull, *International Fuel Performance Experiments (IFPE) Database*, OECD-NEA (2010), http://www.oecd-nea.org/science/fuel/ifpelst.html.
[16] D. Pizzocri, F. Cappia, L. Luzzi, G. Pastore, V.V. Rondinella, P. Van Uffelen, A semi-empirical model for the formation and depletion of the high burnup structure in UO_2, *J. Nucl. Mater.* 487, 23-29 (2017).